

# Magic wavelengths, matrix elements, polarizabilities, and lifetimes of Cs

M. S. Safronova<sup>1,2</sup>, U. I. Safronova<sup>3,4</sup>, and Charles W. Clark<sup>2</sup>

<sup>1</sup>*Department of Physics and Astronomy, 217 Sharp Lab,  
University of Delaware, Newark, Delaware 19716*

<sup>2</sup>*Joint Quantum Institute,  
National Institute of Standards and Technology and the University of Maryland,  
College Park, Maryland 20742*

<sup>3</sup>*Physics Department,  
University of Nevada, Reno, Nevada 89557*

<sup>4</sup>*Department of Physics, University of Notre Dame,  
Notre Dame, IN 46556*

(Dated: March 8, 2022)

Motivated by recent interest in their applications, we report a systematic study of Cs atomic properties calculated by a high-precision relativistic all-order method. Excitation energies, reduced matrix elements, transition rates, and lifetimes are determined for levels with principal quantum numbers  $n \leq 12$  and orbital angular momentum quantum numbers  $l \leq 3$ . Recommended values and estimates of uncertainties are provided for a number of electric-dipole transitions and the electric dipole polarizabilities of the  $ns$ ,  $np$ , and  $nd$  states. We also report a calculation of the electric quadrupole polarizability of the ground state. We display the dynamic polarizabilities of the  $6s$  and  $7p$  states for optical wavelengths between 1160 nm and 1800 nm and identify corresponding magic wavelengths for the  $6s - 7p_{1/2}$ ,  $6s - 7p_{3/2}$  transitions. The values of relevant matrix elements needed for polarizability calculations at other wavelengths are provided.

## I. INTRODUCTION

Cs atoms are used in a wide range of applications including atomic clocks and realization of the second [1, 2], the most precise low-energy test of the Standard Model of the electroweak interactions [3], search for spatiotemporal variation of fundamental constants [4], study of degenerate quantum gases [5], qubits of quantum information systems [6], search for the electric-dipole moment of the electron [7], atom interferometry [8], atomic magnetometry [9], and tests of Lorentz invariance [10]. As a result, accurate knowledge of Cs atomic properties, in particular electric-dipole matrix elements, lifetimes, polarizabilities, and magic wavelengths became increasingly important. While a number of  $6s - np$  and  $7s - np$  transitions have been studied in detail owing to their importance to test of the Standard Model [3], recent applications require reliable values of many other properties.

Many of the applications listed above involve optically trapped Cs atoms. The energy levels of atoms trapped in a light field are generally shifted by a quantity that is proportional to their frequency-dependent polarizability [11]. It is often beneficial to minimize the resulting ac Stark shift of transitions between different levels, for example in cooling or trapping applications. At a “magic wavelength”, which was first used in atomic clock applications [12, 13], the ac Stark shift of a transition is zero. Magic wavelengths for  $6s - 7p$  transitions are of potential use for state-insensitive cooling and trapping and have not been previously calculated. Similar  $2s - 3p$  and  $4s - 5p$  transitions have been recently used in  $^6\text{Li}$  [14] and  $^{40}\text{K}$  [15], respectively, as alternatives to conventional

cooling with the  $2s - 2p$  and  $4s - 4p$  transitions.

Here we report an extensive study of a variety of Cs properties of experimental interest. We use several variants of the relativistic high-precision all-order (linearized coupled-cluster) method [16] to critically evaluate the accuracy of our calculations and provide recommended values with associated uncertainties. Atomic properties of Cs are evaluated for  $ns$ ,  $np$ ,  $nd$ , and  $nf$  states with  $n \leq 12$ . Excitation energies and lifetimes are calculated for the lowest 53 excited states. The reduced electric-dipole matrix elements, line strengths, and transition rates are determined for allowed transitions between these levels. The static electric quadrupole polarizability is determined for the  $6s$  level. Scalar and tensor polarizabilities of  $(5 - 9)d$ ,  $(6 - 9)p$ , and  $(7 - 10)s$  states of Cs are evaluated. The uncertainties of the final values are estimated for all properties.

As a result of these calculations, we are able to identify the magic wavelengths for the  $6s - 7p_{1/2}$  and  $6s - 7p_{3/2}$  transitions in the 1160 nm and 1800 nm wavelength range.

## II. PREVIOUS CS POLARIZABILITY STUDIES

In 2010, Mitroy *et al.* [11] reviewed the theory and applications of atomic and ionic polarizabilities across the periodic table of the elements. The static and dynamic polarizabilities of Cs have increased in interest recently, as demonstrated by a number of experimental [17–29] and theoretical [11, 30–49] studies.

Safronova *et al.* [41] presented results of first-principles calculations of the frequency-dependent polarizabilities

TABLE I: Recommended values of the reduced electric-dipole matrix elements  $D$  in cesium in atomic units. Uncertainties are given in parenthesis. Absolute values are given.

Transition	D	Transition	D	Transition	D	Transition	D	Transition	D
$7s - 6p_{1/2}$	4.24(1)	$6p_{1/2} - 7d_{3/2}$	2.05(2)	$5d_{3/2} - 6p_{1/2}$	7.1(1)	$6d_{3/2} - 6p_{1/2}$	4.23(7)	$5d_{3/2} - 7f_{5/2}$	1.73(1)
$7s - 6p_{3/2}$	6.48(2)	$6p_{3/2} - 7d_{3/2}$	0.976(0)	$5d_{3/2} - 7p_{1/2}$	2.3(4)	$6d_{3/2} - 7p_{1/2}$	17.99(4)	$5d_{3/2} - 8f_{5/2}$	1.34(1)
$7s - 7p_{1/2}$	10.31(4)	$6p_{3/2} - 7d_{5/2}$	2.89(3)	$5d_{3/2} - 8p_{1/2}$	0.63(5)	$6d_{3/2} - 8p_{1/2}$	5.0(2)	$5d_{5/2} - 6f_{5/2}$	0.644(6)
$7s - 7p_{3/2}$	14.32(6)	$6p_{3/2} - 10d_{5/2}$	0.979(6)	$5d_{3/2} - 9p_{1/2}$	0.34(2)	$6d_{3/2} - 9p_{1/2}$	1.56(2)	$5d_{5/2} - 6f_{7/2}$	2.88(3)
$7s - 8p_{1/2}$	0.914(27)	$6p_{3/2} - 11d_{5/2}$	0.782(5)	$5d_{3/2} - 10p_{1/2}$	0.22(1)	$6d_{3/2} - 10p_{1/2}$	0.85(2)	$5d_{5/2} - 7f_{5/2}$	0.468(3)
$7s - 8p_{3/2}$	1.620(35)	$7p_{1/2} - 6d_{3/2}$	17.99(4)	$5d_{3/2} - 11p_{1/2}$	0.164(9)	$6d_{3/2} - 11p_{1/2}$	0.56(1)	$5d_{5/2} - 7f_{7/2}$	2.10(1)
$7s - 9p_{1/2}$	0.349(10)	$7p_{3/2} - 6d_{3/2}$	8.07(2)	$5d_{3/2} - 12p_{1/2}$	0.128(7)	$6d_{3/2} - 12p_{1/2}$	0.415(8)	$6d_{3/2} - 4f_{5/2}$	24.62(9)
$7s - 9p_{3/2}$	0.680(14)	$7p_{3/2} - 6d_{5/2}$	24.35(6)	$5d_{3/2} - 6p_{3/2}$	3.19(7)	$6d_{3/2} - 6p_{3/2}$	2.09(3)	$6d_{5/2} - 4f_{5/2}$	6.60(2)
$7s - 10p_{1/2}$	0.191(6)	$7p_{3/2} - 10d_{3/2}$	0.680(6)	$5d_{3/2} - 7p_{3/2}$	0.9(2)	$6d_{3/2} - 7p_{3/2}$	8.07(2)	$6d_{5/2} - 4f_{7/2}$	29.5(1)
$7s - 10p_{3/2}$	0.396(9)	$7p_{3/2} - 10d_{5/2}$	2.02(2)	$5d_{3/2} - 8p_{3/2}$	0.26(3)	$6d_{3/2} - 8p_{3/2}$	1.98(7)	$7d_{3/2} - 5f_{5/2}$	43.4(2)
$7s - 11p_{1/2}$	0.125(4)	$7p_{3/2} - 11d_{5/2}$	1.55(1)	$5d_{3/2} - 9p_{3/2}$	0.14(1)	$6d_{3/2} - 9p_{3/2}$	0.633(9)	$7d_{5/2} - 5f_{5/2}$	11.66(5)
$7s - 11p_{3/2}$	0.270(7)	$8p_{1/2} - 7d_{3/2}$	32.0(1)	$5d_{3/2} - 10p_{3/2}$	0.091(7)	$6d_{3/2} - 10p_{3/2}$	0.346(7)	$7d_{5/2} - 5f_{7/2}$	52.2(2)
$8s - 7p_{1/2}$	9.31(2)	$8p_{3/2} - 7d_{3/2}$	14.35(5)	$5d_{3/2} - 11p_{3/2}$	0.067(5)	$6d_{3/2} - 11p_{3/2}$	0.230(5)	$8d_{3/2} - 6f_{5/2}$	65.2(5)
$8s - 7p_{3/2}$	14.07(7)	$8p_{3/2} - 7d_{5/2}$	43.2(1)	$5d_{3/2} - 12p_{3/2}$	0.052(4)	$6d_{3/2} - 12p_{3/2}$	0.169(4)	$8d_{5/2} - 6f_{5/2}$	17.5(1)
$8s - 8p_{1/2}$	17.78(6)	$9p_{1/2} - 8d_{3/2}$	49.3(1)	$5d_{5/2} - 6p_{3/2}$	9.7(2)	$6d_{5/2} - 6p_{3/2}$	6.13(9)	$8d_{5/2} - 6f_{7/2}$	78.4(6)
$8s - 8p_{3/2}$	24.56(9)	$9p_{3/2} - 8d_{3/2}$	22.14(7)	$5d_{5/2} - 7p_{3/2}$	2.8(5)	$6d_{5/2} - 7p_{3/2}$	24.35(6)	$9d_{3/2} - 7f_{5/2}$	90.5(9)
$9s - 7p_{1/2}$	1.96(2)	$9p_{3/2} - 8d_{5/2}$	66.6(2)	$5d_{5/2} - 8p_{3/2}$	0.80(7)	$6d_{5/2} - 8p_{3/2}$	6.2(2)	$9d_{5/2} - 7f_{5/2}$	24.4(2)
$9s - 8p_{1/2}$	16.06(4)	$10p_{1/2} - 9d_{3/2}$	70.0(1)	$5d_{5/2} - 9p_{3/2}$	0.43(3)	$6d_{5/2} - 9p_{3/2}$	1.97(3)	$9d_{5/2} - 7f_{7/2}$	108.9(0)
$9s - 8p_{3/2}$	24.13(5)	$10p_{3/2} - 9d_{3/2}$	31.45(8)	$5d_{5/2} - 10p_{3/2}$	0.28(2)	$6d_{5/2} - 10p_{3/2}$	1.07(2)	$10d_{5/2} - 6f_{5/2}$	2.14(2)
$9s - 9p_{1/2}$	27.10(8)	$10p_{3/2} - 9d_{5/2}$	94.5(2)	$5d_{5/2} - 11p_{3/2}$	0.21(1)	$6d_{5/2} - 11p_{3/2}$	0.71(1)	$10d_{5/2} - 6f_{7/2}$	9.56(8)
$9s - 9p_{3/2}$	37.3(1)	$11p_{1/2} - 10d_{3/2}$	94.1(2)	$5d_{5/2} - 12p_{3/2}$	0.16(1)	$6d_{5/2} - 12p_{3/2}$	0.53(1)	$10d_{5/2} - 8f_{5/2}$	32.1(3)
$10s - 7p_{1/2}$	0.999(9)	$11p_{3/2} - 10d_{3/2}$	42.29(9)	$7d_{3/2} - 6p_{1/2}$	2.05(2)	$7d_{5/2} - 6p_{3/2}$	2.89(3)	$10d_{5/2} - 8f_{7/2}$	143(1)
$10s - 8p_{1/2}$	3.15(3)	$11p_{3/2} - 10d_{5/2}$	127.0(2)	$7d_{3/2} - 7p_{1/2}$	6.6(2)	$7d_{5/2} - 7p_{3/2}$	9.6(3)	$11d_{5/2} - 7f_{5/2}$	3.08(3)
$10s - 9p_{1/2}$	24.50(5)	$12p_{1/2} - 11d_{3/2}$	121.6(2)	$7d_{3/2} - 8p_{1/2}$	32.0(1)	$7d_{5/2} - 8p_{3/2}$	43.2(1)	$11d_{5/2} - 7f_{7/2}$	13.8(1)
$10s - 9p_{3/2}$	36.69(8)	$12p_{3/2} - 11d_{3/2}$	54.66(9)	$7d_{3/2} - 9p_{1/2}$	9.0(2)	$7d_{5/2} - 9p_{3/2}$	11.1(2)	$12d_{5/2} - 8f_{5/2}$	4.21(4)
$11s - 7p_{1/2}$	0.650(6)	$12p_{3/2} - 11d_{5/2}$	164.1(2)	$7d_{3/2} - 9p_{3/2}$	3.56(9)	$7d_{5/2} - 10p_{3/2}$	3.6(1)	$12d_{5/2} - 8f_{7/2}$	18.8(2)
$11s - 8p_{1/2}$	1.56(1)	$12s - 8p_{1/2}$	1.002(9)	$7d_{3/2} - 6p_{3/2}$	0.976(0)	$7d_{3/2} - 12p_{3/2}$	0.42(1)	$7d_{3/2} - 8p_{3/2}$	14.35(5)
$11s - 9p_{1/2}$	4.61(4)	$12s - 9p_{1/2}$	2.24(2)	$7d_{3/2} - 7p_{3/2}$	3.3(1)	$7d_{3/2} - 10p_{1/2}$	2.86(8)	$7d_{5/2} - 11p_{3/2}$	1.97(6)
$11s - 9p_{3/2}$	6.29(6)	$13s - 7p_{1/2}$	0.370(3)	$7d_{3/2} - 10p_{3/2}$	1.16(4)	$7d_{3/2} - 11p_{1/2}$	1.55(4)		
$12s - 7p_{1/2}$	0.474(5)	$13s - 8p_{1/2}$	0.727(6)	$7d_{3/2} - 11p_{3/2}$	0.64(2)	$7d_{3/2} - 12p_{1/2}$	1.03(3)		

of all alkali-metal atoms for light in the wavelength range 300-1600 nm, with particular attention to wavelengths of common infrared lasers. High-precision study of Cs polarizabilities for a number of states was presented in Ref. [38]. Inconsistencies between  $5d$  lifetimes and  $6p$  polarizability measurements in Cs was investigated by Safronova and Clark [43]. The *ab initio* calculation of  $6p$  polarizabilities were found to agree with experimental values [43]. An experimental and theoretical study of the  $6d_{3/2}$  polarizability of cesium was reported by Kortyna *et al.* [19]. The scalar and tensor polarizabilities were determined from hyperfine-resolved Stark-shift measurements using two-photon laser-induced-fluorescence spectroscopy of an effusive beam. Auzinsh *et al.* [21] presented an experimental and theoretical investigation of the polarizabilities and hyperfine constants of  $nd$  states in  $^{133}\text{Cs}$ . Experimental values for the hyperfine constant  $A$  were obtained from level-crossing signals of the  $(7, 9, 10)d_{5/2}$  states of Cs and precise calculations of the tensor polarizabilities  $\alpha_2$ . The results of relativistic many-body calculations for scalar and tensor polarizabilities of the  $(5 - 10)d_{3/2}$  and  $(5 - 10)d_{5/2}$  states were presented and compared with measured values from the literature. Gunawardena *et al.* [23] presented results of a

precise determination of the static polarizability of the  $8s$  state of atomic cesium, carried out jointly through experimental measurements of the dc Stark shift of the  $6s \rightarrow 8s$  transition using Doppler-free two-photon absorption and theoretical computations based on a relativistic all-order method.

### III. ELECTRIC-DIPOLE MATRIX ELEMENTS AND LIFETIMES OF CESIUM

We carried out several calculations using different methods of increasing accuracy: the lowest-order Dirac-Fock approximation (DF), second-order relativistic many-body perturbation theory (RMBPT), third-order RMBPT, and several variants of the linearized coupled-cluster (all-order) method. Comparing values obtained in different approximations allows us to evaluate the size of the higher-order correlations corrections beyond the third order and estimate some omitted classes of the high-order correlations correction. As a result, we can present recommended values of Cs properties and estimate their uncertainties. The RMBPT calculations are carried out using the method described in Ref. [50]. A review of

the all-order method, which involves summing series of dominant many-body perturbation terms to all orders, is given in [16]. In the single-double (SD) all-order approach, single and double excitations of the Dirac-Fock orbitals are included. The SDpT all-order approach also includes classes of the triple excitations. Omitted higher excitations can also be estimated by the scaling procedure described in [16], which can be started from either SD or SDpT approximations. We carry out all four of such all-order computations, *ab initio* SD and SDpT and scaled SD and SDpT.

The removal energies for a large number of Cs states, calculated in various approximations are given in Table I of the Supplemental Material [51]. The accuracy of the energy levels is a good general indicator of the overall accuracy of the method. The all-order *ab initio* SD and SDpT values for the ground state ionization potential differ from the experiment [52] by 0.4% and 0.58% respectively. Final *ab initio* SDpT all-order energies are in excellent agreement with experiment, to 0.05-0.4% for all levels with the exception of the  $5d$  states, where the difference is 1.3%-1.4%. The larger discrepancy with experiment for the  $5d$  states is explained by significantly larger correlation corrections, 16% for the  $5d_{3/2}$  state in comparison with only 7% for the  $6p_{1/2}$  state. In the iso-electronic spectra of  $\text{Ba}^+$  and  $\text{La}^{2+}$ , on the other hand, the correlation corrections of  $5d$  and  $6s$  states are comparable [53, 54]. Moreover, triple and higher excitations are significantly larger for the  $5d$  states in comparison to all other states. For example, the difference of the SD and SDpT values is  $398 \text{ cm}^{-1}$  for the  $5d_{3/2}$  state and only  $51 \text{ cm}^{-1}$  for the ground state. As a result, some properties of the  $5d$  states are less accurate than the properties of the other states. The scaling procedure mentioned above is used to correct electric-dipole matrix elements involving  $5d$  states for missing higher excitations.

#### A. Electric-dipole matrix elements

We calculated the  $126 \text{ ns} - n'p$  ( $n = 6 - 14$  and  $n' = 6 - 12$ ),  $168 \text{ np} - n'd$  ( $n = 6 - 12$  and  $n' = 5 - 12$ ), and  $168 \text{ nd} - n'f$  ( $n = 5 - 12$  and  $n' = 4 - 10$ ) transitions. Table I reports those values that make significant contributions to the atomic lifetimes and polarizabilities calculated in the other sections. The absolute values are given in all cases in units of  $a_0 e$ , where  $a_0$  is the Bohr radius and  $e$  is the elementary charge. More details of the matrix-element calculations, including the lowest-order values, are given in Supplemental Material [51].

Unless stated otherwise, we use the conventional system of atomic units, a.u., in which  $e$ , the electron mass  $m_e$ , and the reduced Planck constant  $\hbar$  have the numerical value 1, and the electric constant  $\epsilon_0$  has the numerical value  $1/(4\pi)$ . Dipole polarizabilities  $\alpha$  in a.u. have the dimension of volume, and their numerical values presented here are expressed in units of  $a_0^3$ . The atomic units for  $\alpha$  can be converted to SI units via

TABLE II: Recommended values of radiative lifetimes in nsec). Uncertainties are given in parenthesis and references are given in brackets. The values of lifetimes evaluated in the lowest-order DF approximation are given in column DF to illustrate the importance of the correlation corrections. Experimental and other theoretical values are listed in the two last columns.

Level	DF	Recomm.	Expt.	Other
$6p_{1/2}$	25.4	34.4(1.2)	34.934(94) [55]	
$6p_{3/2}$	22.2	30.0(0.7)	30.460(38) [56]	
$5d_{3/2}$	600	966(34)	909(15) [57]	976 [57]
$5d_{5/2}$	847	1351(52)	1281(9) [57]	1363 [57]
$7s_{1/2}$	45.3	48.4(0.2)	49(4) [58]	56 [58]
$7p_{1/2}$	84	152(18)	155(4) [59]	135 [59]
$7p_{3/2}$	77	128(10)	133(2) [59]	110 [59]
$6d_{3/2}$	153	61(2)	60.0(2.5) [60]	69.9 [60]
$6d_{5/2}$	138	61(2)	60.7(2.5) [60]	64.5 [60]
$8s_{1/2}$	87	93(1)	87(9) [61]	104 [61]
$4f_{7/2}$	25	51(7)	40(6) [58]	43 [58]
$4f_{5/2}$	24	51(7)	40(6) [58]	43 [58]
$8p_{1/2}$	201	376(16)	307(14) [62]	
$8p_{3/2}$	186	320(11)	274(12) [62]	
$7d_{3/2}$	160	95(2)	89(1) [63]	107 [63]
$7d_{5/2}$	151	95(2)	89(1) [63]	107 [63]
$9s_{1/2}$	157	167(2)	159(3) [63]	177 [63]
$5f_{7/2}$	54	96(4)	97(6) [60]	76.8 [60]
$5f_{5/2}$	53	96(4)	95(6) [60]	
$9p_{1/2}$	386	695(19)	575(35) [62]	
$9p_{3/2}$	360	606(16)	502(22) [62]	
$8d_{3/2}$	223	153(3)	141(2) [63]	168 [63]
$8d_{5/2}$	213	153(3)	145(3) [63]	168 [63]
$10s_{1/2}$	262	279(3)	265(4) [63]	293 [63]
$6f_{7/2}$	97	159(3)	149(8) [60]	123.8 [60]
$6f_{5/2}$	96	160(3)		
$10p_{1/2}$	652	1132(29)	920(50) [64]	
$10p_{3/2}$	610	1006(26)	900(40) [64]	
$9d_{3/2}$	321	235(4)	218(3) [63]	257 [63]
$9d_{5/2}$	308	237(4)	217(4) [63]	257 [63]
$11s_{1/2}$	408	434(4)	403(4) [63]	455 [63]
$7f_{7/2}$	158	246(3)	229(15) [60]	189.2 [60]
$7f_{5/2}$	155	248(3)		
$11p_{1/2}$	1012	1702(41)		
$11p_{3/2}$	950	1538(37)		
$10d_{3/2}$	454	348(6)	315(3) [63]	376 [63]
$10d_{5/2}$	439	350(3)	321(4) [63]	376 [63]
$12s_{1/2}$	602	642(6)	573(7) [63]	668 [63]
$8f_{7/2}$	238	361(20)		
$8f_{5/2}$	234	363(6)	336(22) [60]	274.8 [60]
$12p_{1/2}$	1484	2430(55)		
$12p_{3/2}$	1394	2218(52)		
$11d_{3/2}$	626	492(8)	417(5) [63]	529 [63]
$11d_{5/2}$	605	496(5)	420(7) [63]	529 [63]
$13s_{1/2}$	846	901(8)	777(8) [63]	942 [63]
$9f_{7/2}$	340	506(23)	473(30) [60]	385.1 [60]
$9f_{5/2}$	335	511(26)		
$12d_{3/2}$	794	663(24)	566(11) [63]	722 [63]
$12d_{5/2}$	768	661(29)	586(11)	722
$14s_{1/2}$	1033	1087(9)	1017(20) [63]	1282 [63]
$10f_{7/2}$	419	620(27)	646(35) [60]	521.1 [60]
$10f_{5/2}$	414	626(29)		

$\alpha/h$  [Hz/(V/m)<sup>2</sup>]= $2.48832 \times 10^{-8} \alpha$  [a.u.], where the conversion coefficient is  $4\pi\epsilon_0 a_0^3/h$  and the Planck constant  $h$  is factored out.

The estimated uncertainties of the recommended values are listed in parenthesis. The evaluation of the uncertainty of the matrix elements was described in detail in [65, 66]. It is based on four different all-order calculations mentioned in Section III: two *ab initio* all-order calculations with (SDpT) and without (SD) the inclusion of the partial triple excitations and two calculations that included semiempirical estimate of missing high-order correlation corrections starting from both *ab initio* calculations. The spread of these four values was used to estimate uncertainty in the final results for each transition based on the algorithm accounting for the importance of the specific dominant contributions. The largest values of the uncertainties in Table I are for the  $5d - np$  transitions, ranging from 1.9% to 10% for most cases resulting from larger correlation for the  $5d$  states discussed above. The uncertainties are the largest (20%) for the  $5d - 7p$  transitions. Our final results and their uncertainties are used to calculate the recommended values of the lifetimes and polarizabilities discussed below.

## B. Lifetimes

One of the first lifetime measurements in cesium was published by Gallagher [67]. Level crossing measurement of lifetimes in Cs were presented by Schmieder and Lurio [68]. Using a pulsed dye laser and the method of delayed coincidence the lifetime of the  $7p$ ,  $8p$ , and  $9p$  levels were measured by Marek and Niemax [62]. The cascade Hanle-effect technique were used by Budos *et al.* [69] for the lifetime measurements of the  $8s$  and  $9s$  levels. Deech *et al.* [70] reported results of the lifetime measurements made by time-resolved fluorescence from  $ns$  and  $nd_{3/2}$  states of Cs ( $n=8$  to 14) over a range of vapour densities covering the onset of collisional depopulation. The same technique was used by Marek [58] to find out the lifetimes for the  $7s$ ,  $5d$ , and  $4f$  levels. Radiative lifetimes of the  $8s$ ,  $9s$  and  $7d$  levels of Cs were measured by Marek [61] employing the method of delayed coincidences of cascade transitions to levels that cannot be directly excited by electronic dipole transitions from ground state. Alessandretti *et al.* [71] reported measurement of the  $8s$ -level lifetime in Cs vapor, using the two-photon  $6s \rightarrow 8s$  transition. Marek and Ryschka [60] presented lifetime measurements of  $5f - 11f$  levels of Cs using partially superradiant population. Ortiz and Campos [59] measured lifetimes of the  $7p_{1/2}$  and  $7p_{3/2}$  levels of Cs. Neil and Atkinson [63] reported the lifetimes of the  $ns$  ( $n=9-15$ ),  $nd_{3/2}$ , and  $nd_{5/2}$  ( $n=7-12$ ) levels with 1-2% accuracy. Lifetimes were measured by laser-induced fluorescence using two-photon excitation. Small differences between the lifetimes of the different fine-structure levels of each  $nd$  state have been observed for the first time [63]. Bouchiat *et al.* [72] reported measurement of the

TABLE III: Reduced quadrupole matrix elements  $Q$  in a.u. and contributions to quadrupole polarizabilities of the  $6s$  state of cesium in  $a_0^5$ . Uncertainties are given in parenthesis.

Contr.	$Q$	$\alpha_0^{E2}(6s)$
$5d_{3/2}$	33.62	3421(69)
$6d_{3/2}$	12.98	327(21)
$7d_{3/2}$	8.08	109(4)
$8d_{3/2}$	5.53	48(1)
$(9-26)d_{3/2}$		287(1)
$5d_{5/2}$	41.51	5183(88)
$6d_{5/2}$	15.26	452(28)
$7d_{5/2}$	9.64	157(6)
$8d_{5/2}$	6.64	70(2)
$(9-26)d_{5/2}$		379(1)
CORE		86(2)
Total		10521(118)

radiative lifetime of the cesium  $5d_{5/2}$  level using pulsed excitation and delayed probe absorption. Sasso *et al.* [72] reported measurement of the radiative lifetimes and quenching of the cesium  $5d$  levels. Measurement of the  $5d_{5/2}$  lifetime was presented by Hoeling *et al.* [73] and by DiBerardino *et al.* [57].

Precision lifetime measurements of the  $6p$  states in atomic cesium were published in a number of papers by Tanner *et al.* [74], Rafac *et al.* [75], Young *et al.* [55], and Rafac *et al.* [76]. The most accurate result was reported by Rafac *et al.* [75] with lifetimes for  $6p_{1/2}$  ( $34.934 \pm 0.094$  ns) and  $6p_{3/2}$  ( $30.499 \pm 0.070$  ns) states in atomic cesium obtained using the resonant diode-laser excitation of a fast atomic beam to produce those measurements. Recently, lifetime of the cesium  $6p_{3/2}$  state was measured using ultrafast laser-pulse excitation and ionization. The result of Sell *et al.* [56],  $\tau(6p_{3/2}) = 30.460(38)$  ns with an uncertainty of 0.12%, is one of the most accurate lifetime measurements on record.

We calculated lifetimes of the  $(7-14)s$ ,  $(6-12)p$ ,  $(5-12)d$ , and  $(4-10)f$  states in Cs using out final values of the matrix elements listed in Table I and experimental energies from [52]. The uncertainties in the lifetime values are obtained from the uncertainties in the matrix elements listed in Table I. Since experimental energies are very accurate, the uncertainties in the lifetimes originate from the uncertainties in the matrix elements. We also included the lowest-order DF lifetimes  $\tau^{\text{DF}}$  to illustrate the size of the correlation effects, which can be estimated as the differences of the final and lowest-order values. We note that the correlation contributions are large, 5-60%, being 30-40% for most states.

Our results are compared with experiment and other theory. We note that the theoretical results in the “ $\tau^{\text{theory}}$ ” column are generally quoted in the same papers as the experimental measurements, with theoretical values mostly obtained using Coulomb approximation of empirical formulas, which are not expected to be of high accuracy.

We find a 20% difference with the  $8p$  and  $9p$  lifetimes measured by Marek and Niemax [62] using a pulsed dye laser and the method of delayed coincidence. The same technique was used by Marek [58] to measure the lifetimes of the  $7s$  and  $4f$  levels. Our final value is an excellent agreement for the  $7s$  level, and reasonably agree within the combined uncertainties for the  $4f$  levels (51(7) ns vs. 40(6) ns). Radiative lifetime of the  $8s$  level of Cs was measured by Marek [61]. We confirm a good agreement for the  $8s$  level taking uncertainties into account. Our results are in excellent agreements with the Ortiz and Campos [59] measurements for the  $7p_{1/2}$  and  $7p_{3/2}$  lifetimes. We differ by 5% - 10% with the lifetimes of the  $ns$  ( $n = 9 - 15$ ),  $nd_{3/2}$ , and  $nd_{5/2}$  ( $n = 7 - 12$ ) levels reported by Neil and Atkinson [63]. We note that the uncertainties of 1 - 2% quoted in [63] are most likely underestimated. Our lifetimes of the  $6p_{1/2}$  and  $6p_{3/2}$  are in excellent agreements with recent experiment [56] indicating that our uncertainties are overestimated for these levels.

#### IV. STATIC QUADRUPOLE POLARIZABILITIES OF THE $6s$ STATE

The static multipole polarizability  $\alpha^{Ek}$  of Cs in its  $6s$  state can be separated into two terms; a dominant first term from intermediate valence-excited states, and a smaller second term from the core-excited states. The second term is the lesser of these and is evaluated here in the random-phase approximation [77]. The dominant valence contribution is calculated using the sum-over-state approach

$$\alpha_v^{Ek} = \frac{1}{2k+1} \sum_n \frac{|\langle nl_j || r^k C_{kq} || 6s \rangle|^2}{E_{nl_j} - E_{6s}}, \quad (1)$$

where  $C_{kq}(\hat{r})$  is a normalized spherical harmonic and where  $nl$  is  $np$ ,  $nd$ , and  $nf$  for  $k = 1, 2$ , and  $3$ , respectively [78]. Here we discuss the quadrupole ( $k = 2$ ) polarizabilities.

We use recommended energies from [52] and our final quadrupole matrix elements to evaluate terms in the sum with  $n \leq 13$ , and we use theoretical SD energies and matrix elements to evaluate terms with  $13 \leq n \leq 26$ . The remaining contributions to  $\alpha^{E2}$  from orbitals with  $27 \leq n \leq 70$  are evaluated in the random-phase approximation (RPA). We find that this contribution is negligible. The uncertainties in the polarizability contributions are obtained from the uncertainties in the corresponding matrix elements. The final values for the quadrupole matrix elements and their uncertainties are determined using the same procedure as for the dipole matrix elements.

Contributions to the quadrupole polarizability of the  $6s$  ground state are presented in Table III. While the first two terms in the sum-over-states for the electric dipole polarizability contribute 99.5%, the first two terms in the

TABLE IV: The  $\alpha_0$  scalar and  $\alpha_2$  tensor polarizabilities (in multiples of 1000 a.u.) in cesium. Uncertainties are given in parenthesis.

$nl_j$	$\alpha_0$	$nl_j$	$\alpha_2$
$7s_{1/2}$	6.237(42)		
$8s_{1/2}$	38.27(26)		
$9s_{1/2}$	153.7(1.0)		
$10s_{1/2}$	477.5(3.3)		
$11s_{1/2}$	1246(4)		
$12s_{1/2}$	2868(21)		
$13s_{1/2}$	5817(14)		
$6p_{1/2}$	1.339(43)		
$7p_{1/2}$	29.88(16)		
$8p_{1/2}$	223.3(1.4)		
$9p_{1/2}$	1021.4(5.6)		
$10p_{1/2}$	3500(14)		
$11p_{1/2}$	9892(37)		
$12p_{1/2}$	24310(100)		
$6p_{3/2}$	1.651(46)	$6p_{3/2}$	-0.260(11)
$7p_{3/2}$	37.51(17)	$7p_{3/2}$	-4.408(50)
$8p_{3/2}$	284.5(1.7)	$8p_{3/2}$	-30.57(41)
$9p_{3/2}$	1312.9(7.0)	$9p_{3/2}$	-134.7(1.7)
$10p_{3/2}$	4525(20)	$10p_{3/2}$	-451.1(4.8)
$11p_{3/2}$	12836(44)	$11p_{3/2}$	-1254(11)
$12p_{3/2}$	31630(96)	$12p_{3/2}$	-3041(24)
$5d_{3/2}$	-0.335(38)	$5d_{3/2}$	0.357(25)
$6d_{3/2}$	-5.68(12)	$6d_{3/2}$	8.749(78)
$7d_{3/2}$	-66.79(1.0)	$7d_{3/2}$	71.08(75)
$8d_{3/2}$	-369.3(5.8)	$8d_{3/2}$	338.6(3.1)
$9d_{3/2}$	-1405(20)	$9d_{3/2}$	1190(8)
$10d_{3/2}$	-4242(60)	$10d_{3/2}$	3419(22)
$11d_{3/2}$	-10926(149)	$11d_{3/2}$	8511(54)
$12d_{3/2}$	-25092(783)	$12d_{3/2}$	18734(158)
$5d_{5/2}$	-0.439(42)	$5d_{5/2}$	0.677(34)
$6d_{5/2}$	-8.38(13)	$6d_{5/2}$	17.30(11)
$7d_{5/2}$	-88.9(1.3)	$7d_{5/2}$	141.7(1.1)
$8d_{5/2}$	-475.8(6.3)	$8d_{5/2}$	678.1(4.9)
$9d_{5/2}$	-1781(22)	$9d_{5/2}$	2388(14)
$10d_{5/2}$	-5324(59)	$10d_{5/2}$	6871(35)
$11d_{5/2}$	-13615(136)	$11d_{5/2}$	17111(69)
$12d_{5/2}$	-31487(802)	$12d_{5/2}$	38424(291)

sum-over-states for  $\alpha^{E2}$  contribute 82.4%. The first eight terms gives 93.6%. The remaining 6.4% of  $\alpha^{E2}$  contributions are from the  $(9 - 26)nd$  states. Single-photon laser excitation of the  $6s - 5d$  transition has been used in Cs spectroscopy [79], and the transition rate can be calculated from data in Table III.

#### V. SCALAR AND TENSOR POLARIZABILITIES FOR EXCITED STATES OF CESIUM

The frequency-dependent scalar polarizability,  $\alpha(\omega)$ , of an alkali-metal atom in the state  $v$  may be separated into a contribution from the ionic core,  $\alpha_{\text{core}}$ , a core polariz-

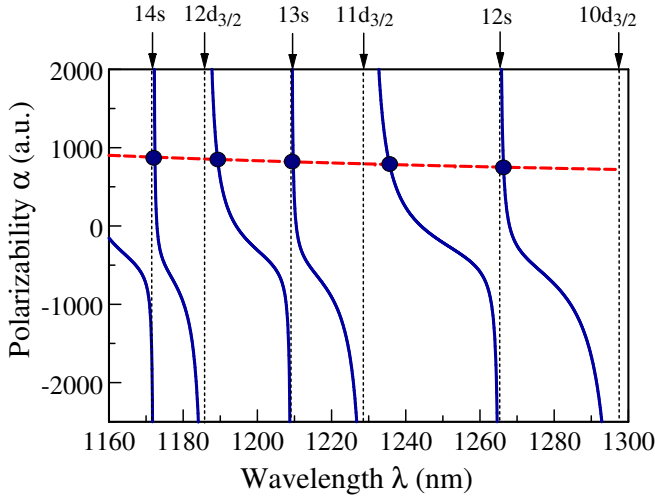


FIG. 1: (Color online) The frequency-dependent polarizabilities of the Cs  $6s$  and  $7p_{1/2}$  states. The magic wavelengths are marked with circles. The approximate positions of the  $7p_{1/2} - nl$  resonances are indicated by vertical lines with small arrows on top of the graph.

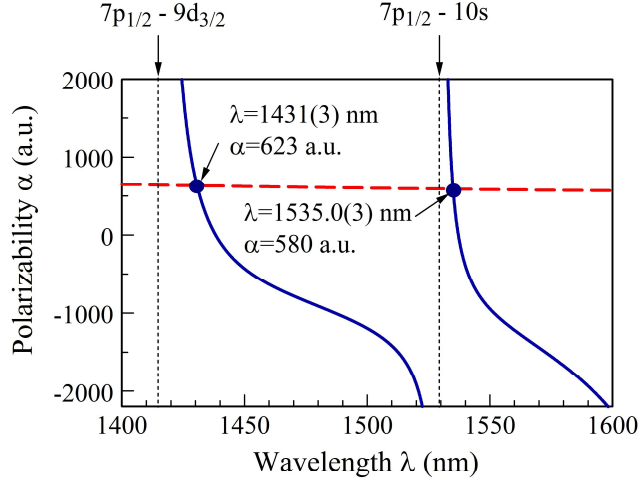
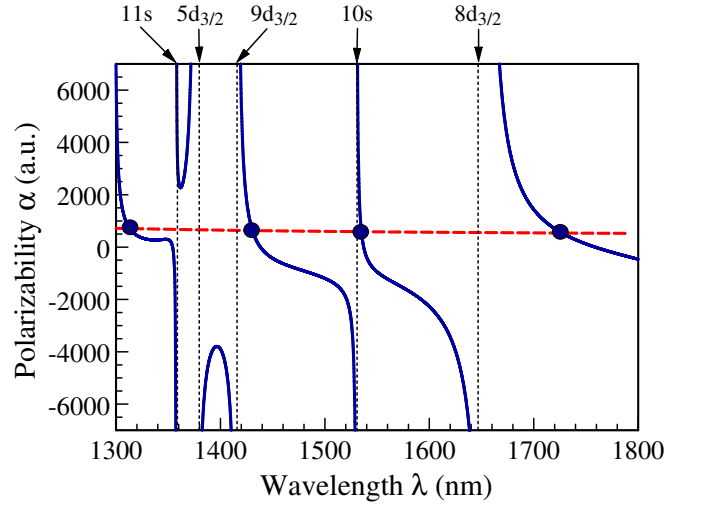


FIG. 2: (Color online) The frequency-dependent polarizabilities of the Cs  $6s$  and  $7p_{1/2}$  states. The magic wavelengths are marked with circles and arrows. The approximate positions of the  $7p_{1/2} - 9d_{3/2}$  and  $7p_{1/2} - 10s$  resonances are indicated by vertical lines with small arrows on top of the graph.

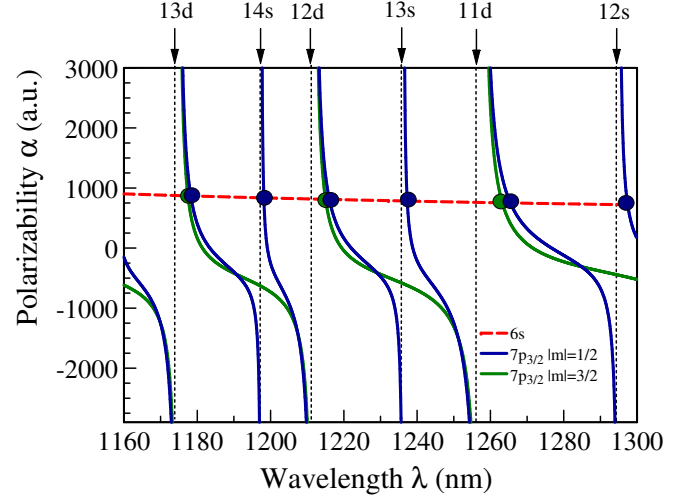


FIG. 3: (Color online) The frequency-dependent polarizabilities of the Cs  $6s$  and  $7p_{3/2}$  states. The magic wavelengths are marked with circles. The approximate positions of the  $7p_{3/2} - nl$  resonances are indicated by vertical lines with small arrows on top of the graph.

ability modification due to the valence electron,  $\alpha_{vc}$ , and a contribution from the valence electron,  $\alpha^v(\omega)$ . We find scalar  $\text{Cs}^+$  ionic core polarizability, calculated in random-phase approximation (RPA) to be  $15.84 a_0^3$ , which is consistent with other data (see Table 4 of Ref. [11]). A counter term  $\alpha_{vc}$  compensates for Pauli principle violating core-valence excitation from the core to the valence shell. It is small,  $\alpha_{vc} = -0.673$  a.u. for the  $6s$  state of Cs. Since the core is isotropic, it makes no contribution to tensor polarizabilities.

The valence contribution to frequency-dependent scalar  $\alpha_0$  and tensor  $\alpha_2$  polarizabilities is evaluated as the

sum over intermediate  $k$  states allowed by the electric-dipole selection rules [11]

$$\begin{aligned} \alpha_0^v(\omega) &= \frac{2}{3(2j_v + 1)} \sum_k \frac{\langle k || D || v \rangle^2 (E_k - E_v)}{(E_k - E_v)^2 - \omega^2}, \\ \alpha_2^v(\omega) &= -4C \sum_k (-1)^{j_v + j_k + 1} \left\{ \begin{matrix} j_v & 1 & j_k \\ 1 & j_v & 2 \end{matrix} \right\} \\ &\quad \times \frac{\langle k || D || v \rangle^2 (E_k - E_v)}{(E_k - E_v)^2 - \omega^2}, \end{aligned} \quad (2)$$

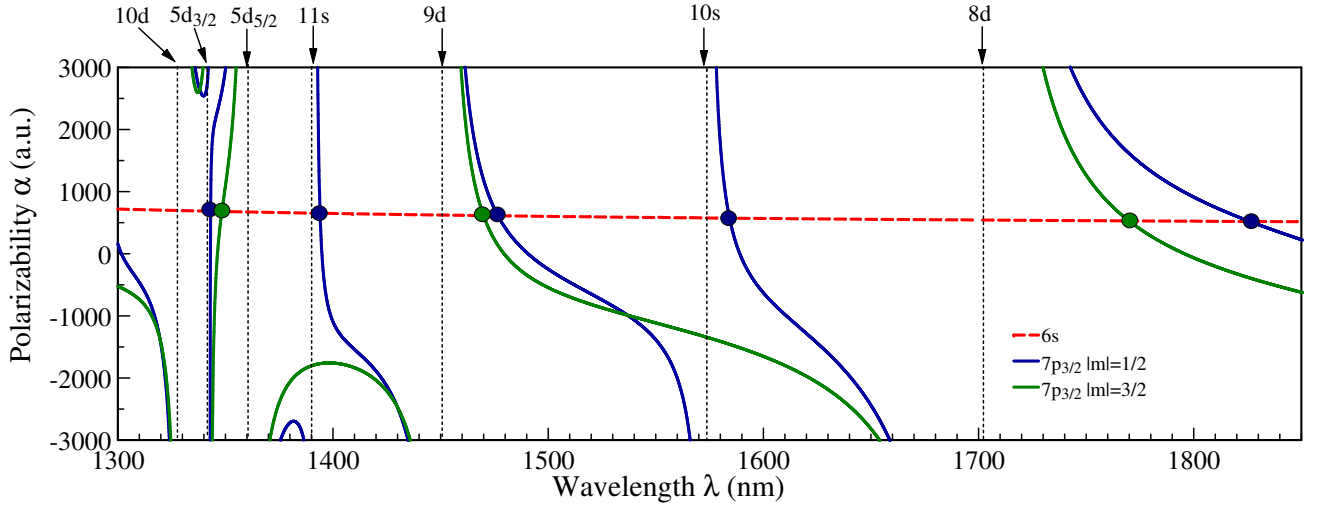


FIG. 4: (Color online) The frequency-dependent polarizabilities of the Cs  $6s$  and  $7p_{3/2}$  states. The magic wavelengths are marked with circles and arrows. The approximate positions of the  $7p_{3/2} - nl$  resonances are indicated by vertical lines with small arrows on top of the graph.

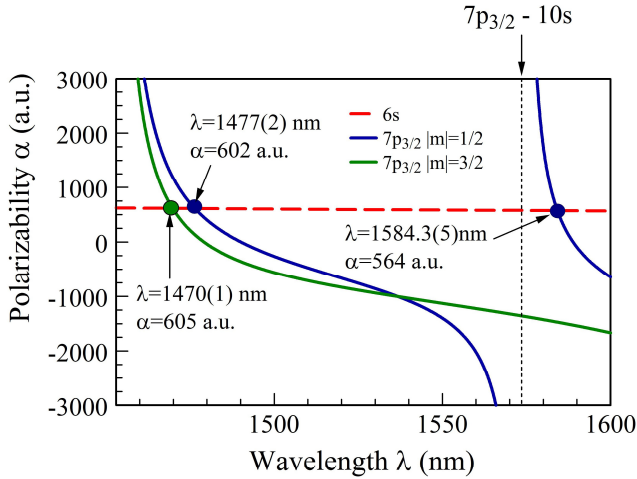


FIG. 5: (Color online) The frequency-dependent polarizabilities of the Cs  $6s$  and  $7p_{3/2}$  states. The magic wavelengths are marked with circles and arrows. The approximate position of the  $7p_{3/2} - 10s$  resonance is indicated by vertical line with small arrows on top of the graph.

where  $C$  is given by

$$C = \left( \frac{5j_v(2j_v - 1)}{6(j_v + 1)(2j_v + 1)(2j_v + 3)} \right)^{1/2}$$

In the equations above,  $\omega$  is assumed to be at least several linewidths off resonance with the corresponding transitions and  $\langle k || D || v \rangle$  are the reduced electric-dipole matrix elements. Linear polarization is assumed in all calculation. To calculate static polarizabilities, we take  $\omega = 0$ . The excited state polarizability calculations are carried out in the same way as the calculations of the multipole polarizabilities discussed in the previous section.

Contributions to the polarizabilities of the  $6p_{1/2}$ ,  $6p_{3/2}$  levels,  $5d_{3/2}$  and  $5d_{5/2}$  state of cesium are given in the Supplemental material [51]. In Table V, we list the  $\alpha_0$  scalar and  $\alpha_2$  tensor polarizabilities (in multiples of 1000 a.u.) in cesium. Uncertainties are given in parenthesis.

The largest (86.6%) contribution to the  $\alpha_0(6p_{1/2})$  value arises from the  $6p_{1/2} - 5d_{3/2}$  transition. The contribution of the  $6s$  and  $7s$  states in the  $\alpha_0(6p_{1/2})$  value nearly cancel each other. Some cancellations are also observed in the breakdown of the  $5d_{3/2}$  polarizability. We find that highly-excited  $(9-26)f$  states contribute significantly, to the  $5d_{3/2}$  and  $5d_{5/2}$  polarizabilities, 14% and 11%, respectively.

We list the scalar polarizabilities of the  $(7-13)s$ ,  $(6-12)np$ , and  $(5-12)d$ , and tensor polarizabilities of the  $(6-12)np_{3/2}$  and  $(5-12)d$  states in Table IV. Uncertainties are given in parenthesis. Comparison with theoretical results from van Wijngaarden and Li [48], Iskrenova-Tchoukova *et al.* [38], and Mitroy *et al.* [11] are given in the Supplemental Material [51]. Results in the review paper [11] are taken from paper [38]. The calculations of Ref. [38] were also obtained using the single-double all-order method. In the present work, we treat higher-excited states more accurately, carrying all-order calculations up to  $n = 26$  instead of  $n = 12$ . As we noted above, higher-excited states are particularly important for the  $nd$  polarizabilities so the only significant differences with results of [11, 38] occur for the  $5d$  polarizabilities.

The scalar and tensor polarizabilities in [48] were evaluated using the Coulomb approximation. The expected scaling of polarizabilities as  $(n^*)^7$ , where  $n^*$  is the effective principal quantum number, was found to hold well for the higher excited states. Our values for the  $n = 11$  and 12 polarizabilities agree to 1% with [48].

TABLE V: Magic wavelengths in nm for the  $6s - 7p$  transitions in Cs in the 1160-1800 nm wavelength range. The corresponding polarizabilities at magic wavelengths are given in a.u. The resonances near the magic wavelengths are listed in the first column.

Resonance	$\lambda_{\text{magic}}$	$\alpha(\lambda_{\text{magic}})$
$6s - 7p_{1/2}$ transition		
$7p_{1/2} - 14s$	1172.40(3)	866
$7p_{1/2} - 12d_{3/2}$	1189.3(4)	838
$7p_{1/2} - 13s$	1209.68(4)	807
$7p_{1/2} - 11d_{3/2}$	1235.7(5)	774
$7p_{1/2} - 12s$	1266.4(1)	740
$7p_{1/2} - 10d_{3/2}$	1313(6)	698
$7p_{1/2} - 9d_{3/2}$	1431(3)	623
$7p_{1/2} - 10s$	1535.0(3)	580
$7p_{1/2} - 8d_{3/2}$	1727(5)	530
$6s - 7p_{3/2},  m  = 1/2$ transition		
$7p_{3/2} - 13d_{3/2}$	1178.3(4)	856
$7p_{3/2} - 14s$	1198.18(4)	824
$7p_{3/2} - 12d_{3/2}$	1216.1(4)	799
$7p_{3/2} - 13s$	1237.31(7)	772
$7p_{3/2} - 11d_{3/2}$	1265.5(8)	741
$7p_{3/2} - 12s$	1297.5(4)	711
$7p_{3/2} - 5d_{3/2}$	11343(2)	675
$7p_{3/2} - 11s$	1394.0(3)	643
$7p_{3/2} - 9d_{3/2}$	1477(2)	602
$7p_{3/2} - 10s$	1584.3(5)	564
$7p_{3/2} - 8d_{3/2}$	1827(6)	512
$6s - 7p_{3/2},  m  = 3/2$ transition		
$7p_{3/2} - 13d_{3/2}$	1177.5(4)	857
$7p_{3/2} - 12d_{3/2}$	1215.0(4)	800
$7p_{3/2} - 11d_{5/2}$	1263.3(5)	743
$7p_{3/2} - 5d_{3/2}$	1348(4)	671
$7p_{3/2} - 9d_{5/2}$	1470(1)	605
$7p_{3/2} - 8d_{5/2}$	1770(3)	521

## VI. MAGIC WAVELENGTHS

Magic wavelengths for  $D_1$  and  $D_2$  lines in alkali-metal atoms were recently investigated in Refs. [80–83]. Flambaum *et al.* [81] considered magic conditions for the ground state hyperfine clock transitions of cesium and rubidium atoms which used as the primary and the secondary frequency standards. The theory of magic optical traps for Zeeman-insensitive clock transitions in alkali-metal atoms was developed by Derevianko [82]. Zhang *et al.* [83] proposed blue-detuned optical traps that were suitable for trapping of both ground-state and Rydberg excited atoms.

Several magic wavelengths were calculated for the  $6s - 6p_{1/2}$  and  $6s - 7p_{3/2}$  transitions in Cs in Ref. [80] using the all-order approach. In this work, we present several other magic wavelengths for the  $6s - 7p_{1/2}$  and  $6s - 7p_{3/2}$  transitions in Cs.

The magic wavelength  $\lambda_{\text{magic}}$  is defined as the wavelength for which the frequency-dependent polarizabilities of two atomic states are the same, leading to a vanishing ac Stark shift for that transition. To determine

magic wavelengths for the  $6s - 7p$  transition, one calculates  $\alpha_{6s}(\lambda)$  and  $\alpha_{7p}(\lambda)$  polarizabilities and finds the wavelengths at which two respective curves intersect. All calculations are carried out for linear polarization.

The frequency-dependent polarizabilities are calculated the same way as the static polarizabilities, but setting  $\omega \neq 0$ . The dependence of the core polarizability on the frequency is negligible for the infrared frequencies of interests for this work. Therefore, we use the RPA static numbers for the ionic core and  $\alpha_{vc}$  terms.

The total polarizability is given by

$$\alpha = \alpha_0 + \alpha_2 \frac{3m^2 - j(j+1)}{j(2j-1)},$$

where  $j$  is the total angular momentum and  $m$  is corresponding magnetic quantum number. The total polarizability for the  $7p_{3/2}$  states is given by

$$\alpha = \alpha_0 - \alpha_2$$

for  $m = \pm 1/2$  and

$$\alpha = \alpha_0 + \alpha_2$$

for the  $m = \pm 3/2$  case. Therefore, the total polarizability of the  $7p_{3/2}$  state depends upon its  $m$  quantum number and the magic wavelengths needs to be determined separately for the cases with  $m = \pm 1/2$  and  $m = \pm 3/2$  for the  $6s - 7p_{3/2}$  transitions, owing to the presence of the tensor contribution to the total polarizability of the  $7p_{3/2}$  state. There is no tensor contribution to the polarizability of the  $7p_{1/2}$  state. To determine the uncertainty in the values of magic wavelengths, we first determine the uncertainties in the polarizability values at the magic wavelengths. Then, the uncertainties in the values of magic wavelengths are determined as the maximum differences between the central value and the crossings of the  $\alpha_{6s} \pm \delta\alpha_{6s}$  and  $\alpha_{7p} \pm \delta\alpha_{7p}$  curves, where the  $\delta\alpha$  are the uncertainties in the corresponding  $6s$  and  $7p$  polarizabilities.

Our magic wavelength results are given by Figs. 1, 2, 3, 4, 5, and Table V. The frequency-dependent polarizabilities of the  $6s$  and  $7p_{1/2}$  states for  $\lambda = 1160 \text{ nm} - 1800 \text{ nm}$  are plotted in Fig. 1. The magic wavelengths occur between the resonances corresponding to the  $7s_{1/2} - nl$  transitions since the  $6s$  polarizability curve has no resonances in this region and is nearly flat. Magic wavelengths are indicated by filled circles. The approximate positions of the  $7s_{1/2} - nl$  resonances are indicated by the lines with small arrows on top of the graph, together with the corresponding  $nl$  label. The  $\lambda = 1160 \text{ nm} - 1800 \text{ nm}$  region contains resonances with  $nl = 5d, 8d - 12d$  and  $nl = 10s - 14s$ . Resonant wavelengths are listed in the last table of the Supplemental Material [51]. The  $5d$  energy levels are below the  $7p$  energy levels, while all of the other levels are above the  $7p$ , leading to interesting features of the  $7p$  polarizability curves near the  $7p - 5d$  resonances. Due to particular experimental interest in

the magic wavelength in the region nearly 1550 nm due to availability of the corresponding laser, we show more detailed plot of the frequency-dependent polarizabilities of the  $6s$  and  $7p_{1/2}$  states in the  $\lambda = 1440 - 1600$  nm region in Fig. 2. The numerical values of these magic wavelengths are given in Table V.

The frequency-dependent polarizabilities of the  $6s$  and  $7p_{3/2}$  states for  $\lambda = 1160$  nm – 1850 nm are plotted in Figs. 3 and 4. The numerical values of these magic wavelengths are given in Table V. A detailed plot of the  $\lambda = 1440 - 1600$  nm region is shown in Fig. 5. With the exception of the  $7p_{3/2} - 5d$  case,  $7p_{3/2} - nd_{3/2}$  and  $7p_{3/2} - nd_{5/2}$  resonances are too close together to show by separate lines on the plots due to small difference in the  $nd_{3/2}$  and  $nd_{5/2}$  energies for large  $n$ . Therefore, we indicate both  $7p_{3/2} - nd_{3/2}$  and  $7p_{3/2} - nd_{5/2}$  resonances by a single vertical line in Figs. 3, 4, and 5 with the “ $nd$ ” label on the top. While there will be additional magic wave-

lengths in between the  $7p_{3/2} - nd_{3/2}$  and  $7p_{3/2} - nd_{5/2}$  resonances, we expect them to be impractical to use in the experiment due to very strong dependence of polarizabilities on the wavelengths in these cases. Therefore, we omit such magic wavelengths in Table V and corresponding figures.

In summary, we carried out a systematic study of Cs atomic properties using all-order methods. Several calculations are carried out to evaluate uncertainties of the final results. Cs properties are needed for interpretation of the current experiments as well as planning of future experimental studies.

This research was performed under the sponsorship of the U.S. Department of Commerce, National Institute of Standards and Technology, and was supported by the National Science Foundation via the Physics Frontiers Center at the Joint Quantum Institute.

- 
- [1] T. P. Heavner, E. A. Donley, F. Levi, G. Costanzo, T. E. Parker, J. H. Shirley, N. Ashby, S. Barlow, and S. R. Jefferts, *Metrologia* **51**, 174 (2014).
  - [2] S. R. Jefferts, T. P. Heavner, T. E. Parker, J. H. Shirley, E. A. Donley, N. Ashby, F. Levi, D. Calonico, and G. A. Costanzo, *Phys. Rev. Lett.* **112**, 050801 (2014).
  - [3] S. G. Porsev, K. Beloy, and A. Derevianko, *Phys. Rev. Lett.* **102**, 181601 (2009).
  - [4] N. Huntemann, B. Lipphardt, C. Tamm, V. Gerginov, S. Weyers, and E. Peik, *Phys. Rev. Lett.* **113**, 210802 (2014).
  - [5] L. W. Clark, L.-C. Ha, C.-Y. Xu, and C. Chin, *Phys. Rev. Lett.* **115**, 155301 (2015).
  - [6] Y. Wang, X. Zhang, T. A. Corcovilos, A. Kumar, and D. S. Weiss, *Phys. Rev. Lett.* **115**, 043003 (2015).
  - [7] C. Tang, T. Zhang, and D. Weiss, in *APS Division of Atomic, Molecular and Optical Physics Meeting Abstracts* (2015).
  - [8] P. Hamilton, M. Jaffe, J. M. Brown, L. Maisenbacher, B. Estey, and H. Müller, *Phys. Rev. Lett.* **114**, 100405 (2015).
  - [9] B. Patton, E. Zhivun, D. C. Hovde, and D. Budker, *Phys. Rev. Lett.* **113**, 013001 (2014).
  - [10] P. Wolf, F. Chapelet, S. Bize, and A. Clairon, *Phys. Rev. Lett.* **96**, 060801 (2006).
  - [11] J. Mitroy, M. S. Safronova, and C. W. Clark, *J. Phys. B* **43**, 202001 (2010).
  - [12] H. Katori, T. Ido, and M. Kuwata-Gonokami, *J. Phys. Soc. Jpn.* **668**, 2479 (1999).
  - [13] J. Ye, D. W. Vernooy, and H. J. Kimble, *Phys. Rev. Lett.* **83**, 4987 (1999).
  - [14] P. M. Duarte, R. A. Hart, J. M. Hitchcock, T. A. Corcovilos, T.-L. Yang, A. Reed, and R. G. Hulet, *Phys. Rev. A* **84**, 061406R (2011).
  - [15] D. C. McKay, D. Jervis, D. J. Fine, J. W. Simpson-Porco, G. J. A. Edge, and J. H. Thywissen, *Phys. Rev. A* **84**, 063420 (2011).
  - [16] M. S. Safronova and W. R. Johnson, *Adv. At. Mol. Opt. Phys.* **55**, 191 (2008).
  - [17] J.-L. Robyr, P. Knowles, and A. Weis, *Phys. Rev. A* **90**, 012505 (2014).
  - [18] D. Antypas and D. S. Elliott, *Phys. Rev. A* **83**, 062511 (2011).
  - [19] A. Kortyna, C. Tinsman, J. Grab, M. S. Safronova, and U. I. Safronova, *Phys. Rev. A* **83**, 042511 (2011).
  - [20] J.-M. Zhao, H. Zhang, Z.-G. Feng, X.-B. Zhu, L.-J. Zhang, C.-Y. Li, and S.-T. Jia, *J. Phys. Soc. Jpn.* **80**, 034303 (2011).
  - [21] M. Auzinsh, K. Bluss, R. Ferber, F. Gahbauer, A. Jarmola, M. S. Safronova, U. I. Safronova, and M. Tamaniš, *Phys. Rev. A* **75**, 022502 (2007).
  - [22] S. Ulzega, A. Hofer, P. Moroshkin, R. Müller-Siebert, D. Nettels, and A. Weis, *Phys. Rev. A* **75**, 042505 (2007).
  - [23] M. Gunawardena, D. S. Elliott, M. S. Safronova, and U. Safronova, *Phys. Rev. A* **75**, 022507 (2007).
  - [24] A. Sieradzian, M. D. Havey, and M. S. Safronova, *Phys. Rev. A* **69**, 022502 (2004).
  - [25] J. M. Amini and H. Gould, *Phys. Rev. Lett.* **91**, 153001 (2003).
  - [26] C. Ospelkaus, U. Rasbach, and A. Weis, *Phys. Rev. A* **67**, 011402 (2003).
  - [27] S. C. Bennett and C. E. Wieman, *Phys. Rev. Lett.* **82**, 2484 (1999).
  - [28] W. Yei, A. Sieradzian, E. Cerasuolo, and M. D. Havey, *Phys. Rev. A* **57**, 3419 (1998).
  - [29] D. Cho, C. S. Wood, S. C. Bennett, J. L. Roberts, and C. E. Wieman, *Phys. Rev. A* **55**, 1007 (1997).
  - [30] A. A. Kamenski and V. D. Ovsiannikov, *J. Phys. B* **47**, 095002 (2014).
  - [31] Y.-B. Tang, C.-B. Li, and H.-X. Qiao, *Chin. Phys. B* **23**, 063101 (2014).
  - [32] B. M. Roberts, V. A. Dzuba, and V. V. Flambaum, *Phys. Rev. A* **88**, 042507 (2013).
  - [33] A. Derevianko, S. G. Porsev, and J. F. Babb, *At. Data Nucl. Data Tables* **96**, 323 (2010).
  - [34] V. A. Dzuba, V. V. Flambaum, K. Beloy, and A. Derevianko, *Phys. Rev. A* **82**, 062513 (2010).
  - [35] D. A. Kondratjev, I. L. Beigman, and L. A. Vainshtein, *J. Russ. Laser Res.* **31**, 294 (2010).
  - [36] E. Y. Il'inova, A. A. Kamenski, and V. D. Ovsiannikov,

- J. Phys. B **42**, 145004 (2009).
- [37] A. Hofer, P. Moroshkin, S. Ulzega, and A. Weis, Phys. Rev. A **77**, 012502 (2008).
- [38] E. Iskrenova-Tchoukova, M. S. Safronova, and U. I. Safronova, J. Comput. Methods Sciences and Eng. **7**, 521 (2007).
- [39] S. Ulzega, A. Hofer, P. Moroshkin, and A. Weis, Europhys. Lett. **76**, 1074 (2006).
- [40] S. G. Porsev and A. Derevianko, Phys. Rev. A **74**, 020502 (2006).
- [41] M. S. Safronova, B. Arora, and C. W. Clark, Phys. Rev. A **73**, 022505 (2006).
- [42] I. S. Lim, P. Schwerdtfeger, B. Metz, and H. Stoll, J. Chem. Phys. **122**, 104103 (2005).
- [43] M. S. Safronova and C. W. Clark, Phys. Rev. A **69**, 040501 (2004).
- [44] S. Magnier and M. Aubert-Frécon, J. Quant. Spectrosc. Radiat. Transfer **75**, 121 (2002).
- [45] M. S. Safronova, W. R. Johnson, and A. Derevianko, Phys. Rev. A **60**, 4476 (1999).
- [46] I. S. Lim, M. Pernpointner, M. Seth, J. K. Laerdahl, P. Schwerdtfeger, P. Neogady, and M. Urban, Phys. Rev. A **60**, 2822 (1999).
- [47] J. Xia, J. Clarke, J. Li, and W. A. van Wijngaarden, Phys. Rev. A **56**, 5176 (1997).
- [48] W. A. van Wijngaarden and J. Li, J. Quant. Spectrosc. Radiat. Transfer **52**, 555 (1994).
- [49] P. Fuentealba and O. Reyes, J. Phys. B **26**, 2245 (1993).
- [50] W. R. Johnson, Z. W. Liu, and J. Sapirstein, At. Data and Nucl. Data Tables **64**, 279 (1996).
- [51] See Supplemental Material at URL for additional Cs data.
- [52] Kramida, A., Ralchenko, Yu., Reader, J., and NIST ASD Team (2014). NIST Atomic Spectra Database (ver. 5.2), [Online]. Available: <http://physics.nist.gov/asd> [2015, September 3]. National Institute of Standards and Technology, Gaithersburg, MD.
- [53] U. I. Safronova and M. S. Safronova, Canadian Journal of Physics **89**, 465 (2011).
- [54] U. I. Safronova and M. S. Safronova, Phys. Rev. A **89**, 052515 (2014).
- [55] L. Young, W. T. H. III, S. J. Sibener, S. D. Price, C. E. Tanner, C. E. Wieman, and S. R. Leone, Phys. Rev. A **50**, 2174 (1994).
- [56] J. F. Sell, B. M. Patterson, T. Ehrenreich, G. Brooke, J. Scoville, and R. J. Knize, Phys. Rev. A **84**, 010501 (2011).
- [57] D. DiBerardino, C. E. Tanner, and A. Sieradzan, Phys. Rev. A **57**, 4204 (1998).
- [58] J. Marek, J. Phys. B **10**, p. L325 (1977).
- [59] M. Ortiz and J. Campos, J. Quant. Spectrosc. Radiat. Transfer **26**, 107 (1981).
- [60] J. Marek and M. Ryschka, Phys. Lett. A **74**, 51 (1979).
- [61] J. Marek, Phys. Lett. A **60**, 190 (1977).
- [62] J. Marek and K. Niemax, J. Phys. B **9**, p. L483 (1976).
- [63] W. S. Neil and J. B. Atkinson, J. Phys. B **17**, 693 (1984).
- [64] A. Sieradzan, W. Jastrzebski, and J. Krasinski, Opt. Commun. **28**, 73 (1979).
- [65] M. S. Safronova and U. I. Safronova, Phys. Rev. A **83**, 052508 (2011).
- [66] M. S. Safronova and U. I. Safronova, Phys. Rev. A **85**, 022504 (2012).
- [67] A. Gallagher, Phys. Rev. **157**, 68 (1967).
- [68] R. W. Schmieder and A. Lurio, Phys. Rev. A **2**, 1216 (1970).
- [69] B. R. Bulos, R. Gupta, and W. Happer, J. Opt. Soc. Am. **66**, 426 (1976).
- [70] J. S. Deech, R. Luypaert, L. R. Pendrill, and G. W. Series, J. Phys. B **10**, p. L137 (1977).
- [71] G. Alessandretti, F. Chiarini, G. Gorini, and F. Petrucci, Opt. Commun. **20**, 289 (1977).
- [72] M. A. Bouchiat, J. Guéna, P. Jacquier, and M. Lintz, Z. Phys. D **24**, 335 (1992).
- [73] B. Hoeling, J. R. Yeh, T. Takekoshi, and R. J. Knize, Opt. Lett. **21**, 74 (1996).
- [74] C. E. Tanner, A. E. Livingston, R. J. Rafac, F. G. Serpa, K. W. Kukla, H. G. Berry, L. Young, and C. A. Kurtz, Phys. Rev. Lett. **69**, 2765 (1992).
- [75] R. J. Rafac, C. E. Tanner, A. E. Livingston, K. W. Kukla, H. G. Berry, and C. A. Kurtz, Phys. Rev. A **50**, p. R1976 (1994).
- [76] R. J. Rafac, C. E. Tanner, A. E. Livingston, and H. G. Berry, Phys. Rev. A **60**, 3648 (1999).
- [77] W. R. Johnson, D. Kolb, and K.-N. Huang, At. Data Nucl. Data Tables **28**, 333 (1983).
- [78] W. R. Johnson, D. R. Plante, and J. Sapirstein, Adv. Atom. Mol. Opt. Phys. **35**, 255 (1995).
- [79] K.-H. Weber and C. J. Sansonetti, Phys. Rev. A **35**, 4650 (1987), URL <http://link.aps.org/doi/10.1103/PhysRevA.35.4650>.
- [80] B. Arora, M. S. Safronova, and C. W. Clark, Phys. Rev. A **76**, 052509 (2007).
- [81] V. V. Flambaum, V. A. Dzuba, and A. Derevianko, Phys. Rev. Lett. **101**, 220801 (2008).
- [82] A. Derevianko, Phys. Rev. A **81**, 051606 (2010).
- [83] S. Zhang, F. Robicheaux, and M. Saffman, Phys. Rev. A **84**, 043408 (2011).